Effect of Powder Bed on Critical Heating Rates for Thermolysis of Ceramic Injection Moldings

Jin-Hua Song, Julian R. G. Evans, and Mohan J. Edirisinghe
Dept. of Materials Technology

E. H. Twizell
Dept. of Mathematics and Statistics
Brunel University, Uxbridge, Middlesex UB8 3PH, United Kingdom

The mass transport during pyrolysis of the degradation product of a polymeric binder used for ceramic molding is analyzed. Two series resistances to transport are incorporated: the diffusion of the product of degradation through its parent polymer during decomposition and the permeation of vapor through a static powder bed used to support the molding. The model predicts the critical rate of heating, Z_c, above which defects caused by boiling of the organic phase occur at the center of the molding. For the system modeled, the permeability of the powder bed has little effect on Z_c if the moldings are small but this is not the case for large moldings where well-packed fine powders should be avoided and the thickness of the powder bed should be kept to a minimum.

Introduction

A range of manufacturing processes which have their origins in polymer technology is now available for the shaping of ceramic and metal artifacts prepared from powder. This range includes injection molding (Edirisinghe and Evans, 1986), extrusion (Wright et al., 1990), vacuum forming (Haunton et al., 1990), blow molding (Hammond and Evans, 1991), melt spinning (Cass, 1991), solvent casting (Richerson, 1992), and film blowing (Greener and Evans, 1993).

The powder is incorporated in an organic vehicle which often consists of a polymer or blend of polymers and waxes to produce a binary pore-free composite with powder volume fractions typically in the range of 0.5–0.7. Shape is created by taking advantage of the shear and extensional flow properties of the molten suspension. The organic vehicle is then removed and the remaining assembly of particles is sintered following the same procedures that could be used if the powder had been assembled by conventional compaction.

This article addresses the difficult process of removing the organic vehicle without disrupting the assembly of particles. Although special organic compositions can be removed by solvent treatment, by capillary flow into a powder bed, or by low temperature catalytic degradation, the most favored approach is to use controlled thermolysis. The artifact is often supported in a powder bed to prevent slumping as it is heated.

Under these conditions, it is necessary to identify the mass transport paths by which the organic vehicle departs from the powder assembly. Low molecular weight organic species are lost by evaporation, initially from the outer surface but subsequently from internal surfaces once continuous porosity has developed. In oxidizing environments, oxidative chain scission takes place in the surface region and evaporation of fragments occurs from the surface. Activation energy measurements can identify these processes (Wright et al., 1989). In both these situations, and in the case of moldings which are heated in a nonoxidizing atmosphere, thermal degradation takes place throughout the body generating low molecular weight fragments. Activation energy measurements also confirm this (Wright et al., 1989). The problem is that in the early stages, before continuous porosity has formed, the only path available for mass transport of thermal degradation products is diffusion in the parent polymer, which forms the continuous phase, to the surface where evaporation can take place. In a large molding, or in a small molding heated rapidly, this is the critical stage for the formation of defects which occur by boiling of the solution of degradation products. This gives rise to bloating of thick sections (Zhang et al., 1989).

Mathematical models have been developed which describe the competition between the generation of degradation products and their diffusion to the surface so that conditions can be devised to transcend this difficult stage in the thermolysis

process (Calvert and Cima, 1990; Evans et al., 1991). These models necessarily take a simple system where the organic vehicle consists of a single polymer which decomposes to monomer. This is because in a multiproduct degradation, each product influences the diffusion coefficient of every other product through free volume effects.

These models have been experimentally tested (Evans et al., 1991; Matar et al., 1996) and assume that the surface mass transport coefficient is infinite leading to a zero surface concentration, which is used as the boundary condition. Since the heating rates studied are very low and a sweep of nonoxidizing gas carries away the vapor, this assumption is acceptable.

The resistance to vapor transport is likely to be higher if the artifact is packed in a powder bed for support. If the organic vehicle is of low molecular weight, it may flow into the surrounding powder and the kinetics of this partitioning have been studied (Bao and Evans, 1991). In the case of a polymeric binder, however, little fluid flow occurs and the effect of the powder bed is to offer a resistance to vapor transport in the early stage of the thermolysis. This means that the boundary condition can no longer be taken as zero, but rather a variable boundary condition must be employed which depends on the flux of monomer and the resistance to gas transport in the powder bed. The particle size, packing efficiency, and dimensions of the powder bed are the principal variables that influence this resistance and their effects are studied here.

Theory

A molding in the form an infinite cylinder of radius r_o (m) containing a powder at volume fraction V_c $(0 < V_c < 1)$ in polyalphamethylstyrene is embedded in a powder bed which is a cylindrical annulus with an outer radius r_b (m) and the polymer is removed by pyrolysis by heating at a constant rate, Z. The polymer degrades exclusively to monomer (Evans et al., 1991), which diffuses through the parent polymer-powder composite. Several polymers degrade exclusively to monomer, among them polyoxymethylene, short ester group acrylics, and polyalphamethylstyrene. A monomer concentration profile is developed throughout the molding and powder bed, while at the outer surface of the powder bed the degradation product is flushed by a sweep gas making the monomer concentration at this surface approximate to zero. The major objective is to determine the highest possible heating rate known as the critical heating rate (Z_c) at which the peak monomer vapor pressure at the center of the cylinder does not exceed the ambient pressure. In this way, no defects due to boiling may occur. Figure 1 shows the geometry of the molding and the powder bed. The small shrinkage of the cylinder associated with loss of organic vehicle is neglected, and r_0 is taken as a constant.

In the simplest model which shows close agreement with experimental results (Evans et al., 1991; Matar et al., 1996) and is used here, the effect of loss of polymer on the transport coefficient is neglected and hence the worst case is examined. The development of porosity as the polymer is lost can take two extreme forms; either distributed discontinuous porosity develops or the remaining polymer withdraws to the center leaving a porous outer shell in the molding (Matar et al., 1993). These two extreme cases, together with the coexistence of distributed porosity and a porous shell have been studied to create Z_c-porosity maps at different ceramic volume fractions (Shaw and Edirisinghe, 1995). It is shown that porosity increases the predicted critical rate for a cylindrical molding by a maximum factor of 2.7. Once the percolation threshold is reached and continuous porosity develops, fast gas transport paths become available in the molding and dramatic increases in heating rate are possible. The present work addresses the critical early stages of the pyrolysis of organic vehicle before porosity develops.

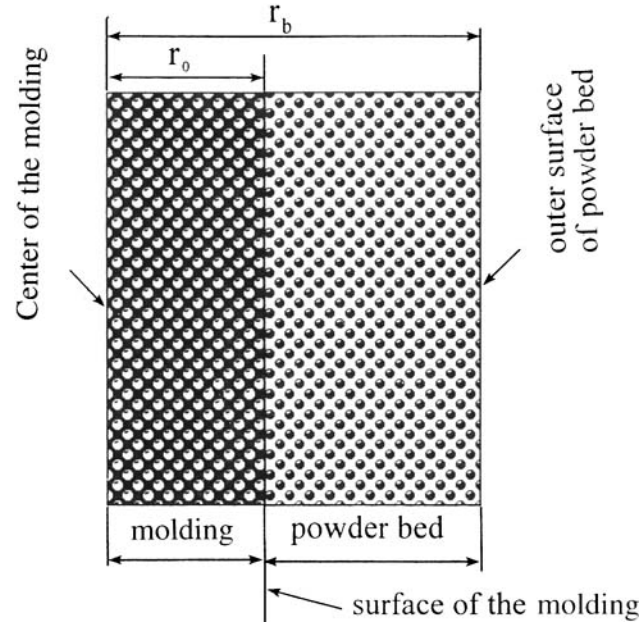

Figure 1. Geometry of the molding and surrounding powder bed.

A cylindrical molding of infinite length is considered.

The monomer concentration, C, throughout the molding can be found from the solution of the partial differential equation written for variable diffusion coefficient since, in weakly bonded thermoplastic polymers, D can vary over five orders of magnitude with concentration of diffusant:

$$\frac{\partial C}{\partial t} = \frac{1}{r}\frac{\partial}{\partial r}\left(rD\frac{\partial C}{\partial r}\right) + \dot{Q}. \tag{1}$$

The diffusion coefficient D $(m^2 \cdot s^{-1})$ varies with temperature, monomer concentration, and powder volume fraction (Matar et al., 1993) and can be found by combining the free volume equation of Duda et al. (1982) with Maxwell's equation for transport in a dispersed system where diffusion in the dispersed phase is zero. This gives rise to Eq. 2 (Matar et al., 1993)

$$D = \left(1 - \frac{3V_c}{V_c + 2}\right) D_0 \exp\left(-\frac{E_D}{RT}\right)(1-\phi)^2 \cdot (1 - 2\chi\phi) \cdot \exp\left\{-[W_1 V_1(0) + W_2 \xi V_2(0)]\frac{\omega}{V_f}\right\}, \tag{2}$$

The details of the calculation for the term ω/V_f using WLF theory has been given by Evans et al. (1991). Values of D_o (preexponential factor) in $m^2 \cdot s^{-1}$ and E_D (activation energy for diffusion) in $J \cdot mol^{-1}$ are taken from the similar system ethylbenzene-polystyrene (Duda et al., 1982), because the experimental determinations for alphamethylstyrene in its polymer are confounded by polymerization effects. $\dot{Q}$ is the rate of production of the monomer based on the total volume of the powder-polymer suspension ($kg \cdot m^{-3} \cdot s^{-1}$) (Matar et al., 1991) and is calculated using the procedure of Reich and Stivala (1971) by

$$\dot{Q} = \rho_p V_p K_0 \exp[-E/(RT)] \cdot \exp\left\{-\frac{K_0 RT^2 \exp[-E/(RT)]}{ZE}\left[1-\frac{2RT}{E}+\frac{6(RT)^2}{E^2}\right]\right\} \quad (3)$$

Equation 1 is solved using a fully implicit finite difference method, details of which are given by Twizell (1984). The finite difference mesh is shown in Figure 2. The initial concentration is $C_{i,0} = 0$ $(i = 0,1,2,3 \ldots N)$ and the concentration profiles at time level j $(j = 1,2,3 \ldots M)$ are found by solving the following system of equations

$$\begin{bmatrix} \beta_{0,j} & \gamma_{0,j} & & & & & \\ \alpha_{1,j} & \beta_{1,j} & \gamma_{1,j} & & & & \\ & \alpha_{2,j} & \beta_{2,j} & \gamma_{2,j} & & & \\ & & \cdot & \cdot & \cdot & & \\ & & & \cdot & \cdot & \cdot & \\ & & & & \alpha_{N-2,j} & \beta_{N-2,j} & \gamma_{N-2,j} \\ & & & & & \alpha_{N-1,j} & \beta_{N-1,j} \end{bmatrix} \cdot \begin{bmatrix} C_{0,j} \\ C_{1,j} \\ C_{2,j} \\ \cdot \\ \cdot \\ C_{N-2,j} \\ C_{N-1,j} \end{bmatrix} = \begin{bmatrix} b_{0,j} \\ b_{1,j} \\ b_{2,j} \\ \cdot \\ \cdot \\ b_{N-2,j} \\ b_{N-1,j} \end{bmatrix}, \quad (4)$$

where

$$\alpha_{i,j} = -\frac{g\left(i-\frac{1}{2}\right)D_{i-\frac{1}{2},j}}{i}, \quad (i = 1,2,3, \ldots N-1) \quad (5)$$

$$\beta_{0,j} = 1 + 4gD_{i=0,j} \quad (6)$$

$$\beta_{i,j} = 1 + \frac{g\left(i-\frac{1}{2}\right)D_{i-\frac{1}{2},j}}{i} + \frac{g\left(i+\frac{1}{2}\right)D_{i+\frac{1}{2},j}}{i}, \quad (i = 1,2,3, \ldots N-1) \quad (7)$$

$$\gamma_{0,j} = -4gD_{i=0,j} \quad (8)$$

$$\gamma_{i,j} = -\frac{g\left(i+\frac{1}{2}\right)D_{i+\frac{1}{2},j}}{i}, \quad (i = 1,2,3, \ldots N-2) \quad (9)$$

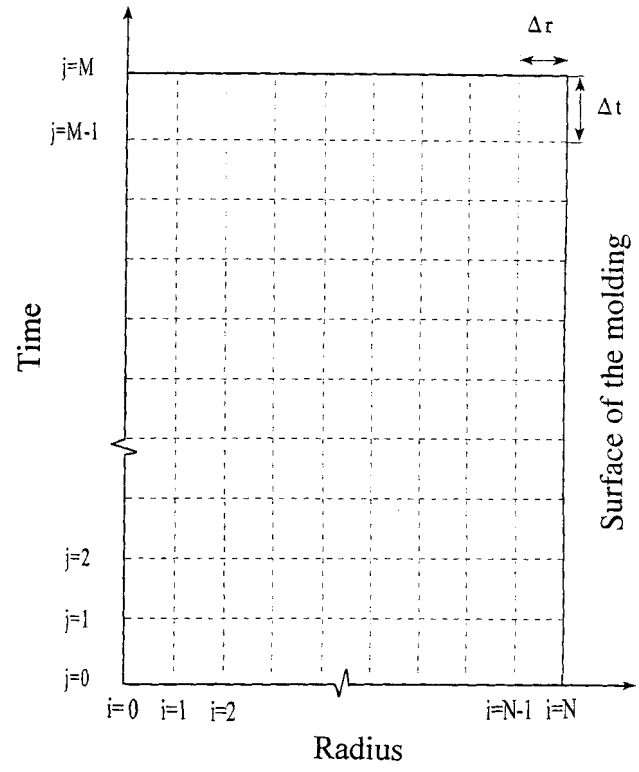

Figure 2. Grid of time and radius space for the finite difference method.

$$b_{i,j} = C_{i,j-1} + \frac{\Delta t}{2}\left(\dot{Q}_{i,j} + \dot{Q}_{i,j-1}\right), \quad (i = 0,1,2,3, \ldots N-2) \quad (10)$$

$$b_{N-1,j} = C_{N-1,j-1} + \frac{\Delta t}{2}\left(\dot{Q}_{N-1,j-1} + \dot{Q}_{N-1,j}\right) + \frac{g\left(N-\frac{1}{2}\right)D_{N-\frac{1}{2},j}}{N-1}C_{N,j} \quad (11)$$

and

$$g = \frac{\Delta t}{(\Delta r)^2} \quad (12)$$

When a powder bed is present, the solution requires the value of the boundary monomer concentration $C_{N,j}$ ($kg \cdot m^{-3}$) at the surface of the molding of radius r_0. The mass fraction of polymer remaining at a given temperature $T = j\Delta T + T_0$ is calculated using the procedure of Reich and Stivala (1971) as

$$h = \exp\left\{-\frac{K_0 RT^2 \exp\left[-\frac{E}{RT}\right]}{ZE}\left[1-\frac{2RT}{E}+\frac{6(RT)^2}{E^2}\right]\right\} \quad (13)$$

The boundary concentration is zero for the first time step ($j=1$). For the subsequent time steps ($j \geq 2$), $C_{N,j}$ is time dependent and is found from the monomer vapor pressure developed at the surface of the molding using Darcy's equation (Scheidegger, 1975) for flow of monomer in the gaseous state through the powder bed of thickness $r_b - r_0$

$$\frac{dv}{dt} = -\frac{K_b}{\eta}\frac{dp}{dr}, \tag{14}$$

where dv/dt is the volume flux of monomer per unit area at radius r ($r_0 \leq r \leq r_b$) given by

$$\frac{dv}{dt} = \frac{w_{j-1}\,\zeta\,T_{j-1}}{2\pi r\,\Delta t\,M_w} \tag{15}$$

in which $\zeta = 8.2\times10^{-5}$ m$^3\cdot$mol$^{-1}\cdot$K^{-1} is a constant derived from Charles' law. In Eq. 15, M_w is the molecular weight (kg$\cdot$mol^{-1}) and w_{j-1} is the mass of monomer displaced from a unit length of cylinder during the previous time step $j-1$ given by

$$w_{j-1} = (h_{j-2} - h_{j-1})(1-V_c)\rho_p \pi r_0^2 - \left[\sum_{i=1}^{N} C_{i,j-1}\pi\left(r_{i+1,j-1}^2 - r_{i,j-1}^2\right) - \sum_{i=1}^{N} C_{i,j-2}\pi\left(r_{i+1,j-2}^2 - r_{i,j-2}^2\right)\right]. \tag{16}$$

In Eq. 14, η is the viscosity of the vapor at a given temperature. For alphamethylstyrene, an equation developed using the Chapman-Enskog theory (Birch, 1976) can be used to calculate the viscosity. This equation is

$$\eta_{j-1} = \frac{5m}{16\sigma^2}\sqrt{\frac{RT_{j-1}}{\pi}}, \tag{17}$$

where $m = 1.962\times10^{-25}$ kg is the mass of one molecule of alphamethylstyrene and $\sigma = 6.27\times10^{-10}$ m; σ is the collision diameter of the molecule. This was calculated from the van der Waal's molecular volume using group contributions and assuming sphericity (Bondi and Simkin, 1960). Integrating Eq. 14 through the powder bed of thickness ($r_b - r_0$) using the permeability coefficient K_b(m^2), the boundary vapor pressure at r_0 is obtained as

$$p_j = \frac{w_{j-1}\,\zeta\,T_{j-1}\eta_{j-1}}{2\pi\,\Delta t\,M_w\,K_b}\ln\left(\frac{r_b}{r_0}\right) = \left(\frac{dv}{dt}\right)_{r_0}\frac{\eta_{j-1}r_0}{K_b}\ln\left(\frac{r_b}{r_0}\right) \tag{18}$$

The boundary concentration $C_{N,j}$ can then be found by assuming that by the end of each time step the vapor adjacent to the boundary is in equilibrium with its solution in the continuous phase (Maddox and Hines, 1985) and is given by the equation

$$C_{N,j} = W_1\,\rho_p(1-V_c). \tag{19}$$

Here W_1, the weight fraction of monomer in polymer ($0 < W_1 < 1$) is deduced from θ_1 ($0 < \theta_1 < 1$), the volume fraction of monomer just beneath the boundary, which is the root of the equation

$$p_j = p_1^0\theta_1\exp\left[(1-\theta_1) + \chi(1-\theta_1)^2\right] \tag{20}$$

in which

$$p_1^0 = \exp\left(-\frac{\Delta H_{\text{vap}}}{RT} + I\right). \tag{21}$$

The root θ_1 can be found numerically in the region $0 \leq \theta_1 \leq 1$ using the gold-sectioning method (Press et al., 1986). Strictly, Eq. 19 should employ the density of the monomer-polymer solution but since the monomer is present at only a few percent, the density of polymer is used. Since the densities of monomer and polymer are close, $W_1 \approx \theta_1$. However, this approximation introduces an error when the resistance to gas transport is high such as for radii of powder bed greater than five times the radius of the molding at $K_b = 10^{-14}$ m^2.

Having found $C_{N,j}$, the system of Eqs. 4 can be solved using an LU-decomposition method (Forsythe and Moler, 1967) for the monomer concentration profile at time level j. Programming was in FORTRAN 77 (see the Appendix) and the calculations were carried out on a UNIX system. The values for the parameters of degradation and diffusion equations are listed in Table 1 (Evans et al., 1991).

Results and Discussion

It has been assumed in earlier work (Evans et al., 1991; Matar et al., 1993) that the resistance to the gas transport at the surface of the molding was negligible so that zero monomer concentration ($C_{N,j} = 0$) could be applied at any time level j. Table 2 shows the critical heating rates calculated under this assumption for cylinders with a range of radii. Clearly the thicker a cylinder, the lower the critical heating rate must be to avoid boiling. This zero boundary condition is reasonable, however, only when the gas transport resistance through the powder bed is negligibly low so that no significant boundary vapor pressure p_j (Pa) can be established.

During pyrolysis, the concentration of monomer at the center first rises as the rate of decomposition of polymer accelerates and then falls as the amount of residual polymer becomes depleted. There is a corresponding maximum in the equilibrium vapor pressure associated with this solution. Curve a in Figure 3 shows the predicted radial monomer concentration at the temperature at which the vapor pressure over the solution at the center reaches this maximum. This temperature is denoted by T_c. The curves in Figure 3 are calculated for the critical heating rate $Z_c = 1.93\times10^{-3}$ K$\cdot$s^{-1}. The boundary monomer concentration was assumed to be zero for curve a in Figure 3 ($C_{N,j} = 0$). The concentration at the center thus corresponds to a vapor pressure just below ambient pressure where boiling is just prevented. Curves b and c in Figure 3 show how a nonzero boundary condition affects this concentration profile. The value of $C_{N,j}$ was fixed at 4 and 8 kg$\cdot$m^{-3} throughout the heating schedule while

Table 1. Parameters Used in the Computation

Quantity	Value	Units	Reference
D_0	6.92×10^{-4}	m^2s^{-1}	Duda et al. (1978)
E	222,000	$J\cdot mol^{-1}$	Evans et al. (1991)
E_d	38,370	$J\cdot mol^{-1}$	Duda et al. (1978)
ΔH_{vap}	38,940	$J\cdot mol^{-1}$	Evans et al. (1991)
I	22.255	Pa	Evans et al. (1991)
K_0	1.67×10^{-16}	s^{-1}	Evans et al. (1991)
m	1.962×10^{-25}	kg	This work
M	620	—	This work
M_w	0.1181	$kg\cdot mol^{-1}$	Evans et al. (1991)
N	100	—	This work
$V_1(0)$	8.686×10^{-4}	$m^3\cdot kg^{-1}$	Coulter and Kehde (1970)
$V_2(0)$	7.975×10^{-4}	$m^3\cdot kg^{-1}$	Endo et al. (1969)
V_c	0.5	—	This work
Δt	0.5	s	This work
T_0	393	K	This work
ξ	0.54	—	Evans et al. (1991)
χ	0.361	—	Canagaratne et al. (1966)
σ	6.27×10^{-10}	m	This work
ζ	8.2×10^{-5}	$m^3\cdot mol^{-1}\cdot K^{-1}$	This work
ω/V_f	variable	$kg\cdot m^{-3}$	Calculated using the method of Duda et al. (1982) from data in Evans et al. (1991)

other conditions remained unchanged. The central concentrations correspond to vapor pressures well above the ambient pressure and hence boiling takes place. To avoid this happening, the heating rate must be lowered and a new value of Z_c found.

A relative critical heating rate is defined as the ratio of $(Z_c)_b$, the critical heating rate when a powder bed is present and the boundary vapor pressure is given by Eq. 18, to $(Z_c)_0$ as defined earlier for the case of a boundary condition fixed at zero throughout the pyrolysis. Thus the ratio $(Z_c)_b/(Z_c)_0$ represents the effect of powder bed [$(Zc)_b/(Zc)_0 = 1$ when the powder bed is absent or its effect is negligible]. Figure 4 shows the relative critical heating rate vs. relative powder bed thickness r_b/r_0 for a cylinder with $r_0 = 5.0$ mm and a range of K_b values. At high powder-bed permeability coefficients (such as $K_b = 10^{-12}$ m^2 in Figure 4), the relative critical heating rates are almost unaffected regardless of the powder bed thickness showing that the resistance to gas transport in the powder bed is negligible compared with the resistance to transport of monomer by diffusion in molten polymer within the molding. However, at low powder bed permeability coefficients (such as $K_b = 10^{-14}$ m^2 in Figure 4) the relative heating rate decreases much more rapidly as the powder bed thickness increases.

The size of the molding also influences the boundary conditions. At a given temperature and heating rate, the flux at the molding surface is proportional to the radius of the molding, r_0, if the mass of monomer stored in solution in the molding is neglected by comparison with that expelled (Eqs. 15 and 16). Figure 5 shows the calculated flux, which deviates only slightly from a linear dependence on radius because the stored mass is extremely small. Therefore, as shown by Eq. 18, a thicker molding gives rise to a higher boundary vapor pressure which affects the monomer concentration at the center of molding, as shown by Figure 3. Consequently, the heating rate for a thicker molding has to be lowered to avoid boiling. This is shown in Figure 6a where the powder bed permeability coefficient is $K_b = 10^{-13}$ m^2. For thinner cylinders, the relative critical heating rates are not sensitive to powder bed thickness but the ratio drops significantly as powder bed thickness increases for thicker cylinders. This dependency on molding thickness is more explicit for low permeability coefficients. Figure 6b shows the effect of the powder bed when $K_b = 10^{-14}$ m^2. Compared with Figure 6a, the relative critical heating rates are much more sensitive to the relative powder bed thickness, especially for thicker moldings. For instance, it would be extremely difficult to remove

Table 2. Critical Heating Rates Calculated Assuming Zero Boundary Monomer Concentration*

r_0 (mm)	1.25	2.5	5.0	10.0
$(Z_c)_0$ ($K\cdot s^{-1}$)	1.30×10^{-3}	1.92×10^{-4}	3.06×10^{-5}	5.56×10^{-6}

*A powder bed is absent.

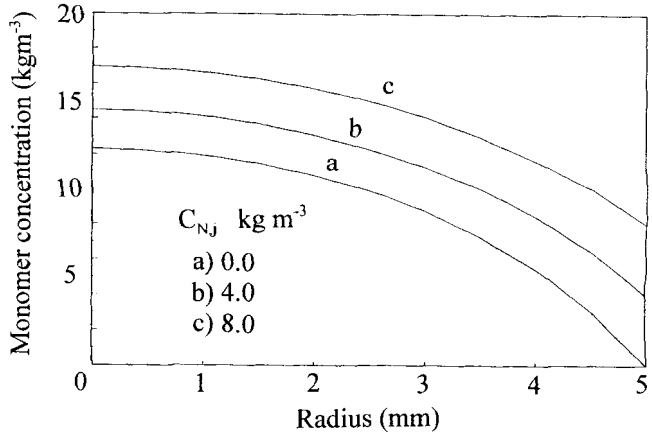

Figure 3. Effect of boundary monomer concentration $C_{N,j}$ on the overall concentration profiles.
$r_0 = 2.5$ mm, $Z_c = 1.92\times10^{-4}$ K·s^{-1}, $T_c = 549$ K.

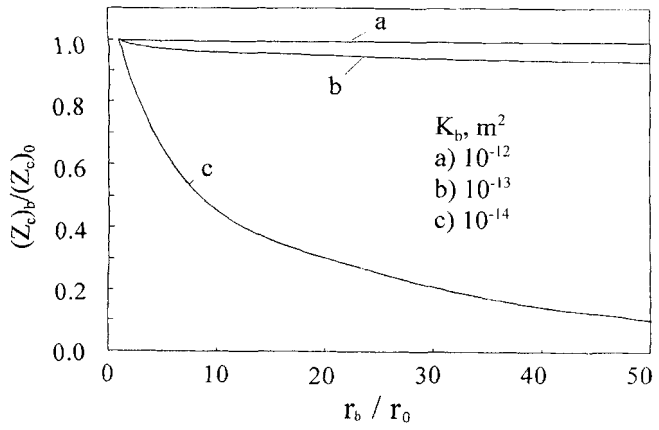

Figure 4. Effect of powder bed permeability (K_b) on the relative critical heating rate, $(Z_c)_b/(Z_c)_0$ for a cylinder of $r_0 = 5.0$ mm.

binder from a molding with a radius of 10 mm if the powder bed thickness reaches 10 mm (see curve d in Figure 6b). For practical purposes, however, such a low powder bed permeability coefficient ($K_b < 10^{-13}$ m^2) is generally very rare for reasons discussed below.

In order not to cause damage to the moldings, the powder bed must only be compacted to a low packing fraction while the molding is being embedded and this means that its packing efficiency (true volume/apparent volume) is likely to be close to that deduced from the tap density (ASTM Designation C 520-81). Typical packing efficiencies are in the range of 24–45% depending on particle properties such as size, size distribution, and shape. Bao and Evans (1991) measured permeability coefficients of powder beds made from four diverse alumina powders, and values were in the range of 10^{-13}–10^{-11} m^2. It has also been shown in their work that, although many equations have been proposed in an attempt to calculate the permeability coefficient from easily measured parameters such as particle size and packing efficiency, there

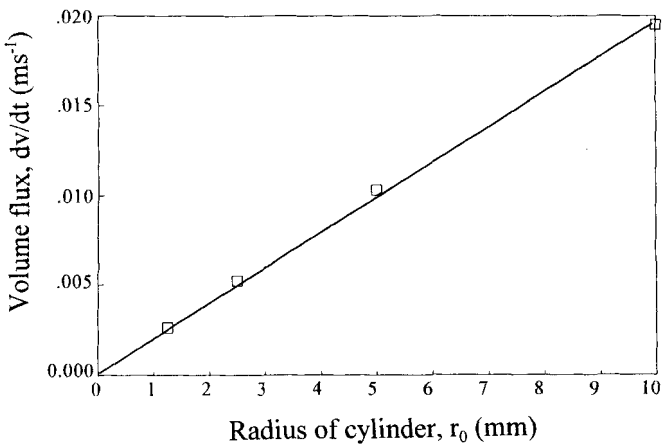

Figure 5. Relationship between volume flux per unit area (dv/dt) at r_0 for unit length of cylinder and cylinder radius.

$Z_c = 3.06 \times 10^{-5}$ K·s^{-1}, $T = 520$ K.

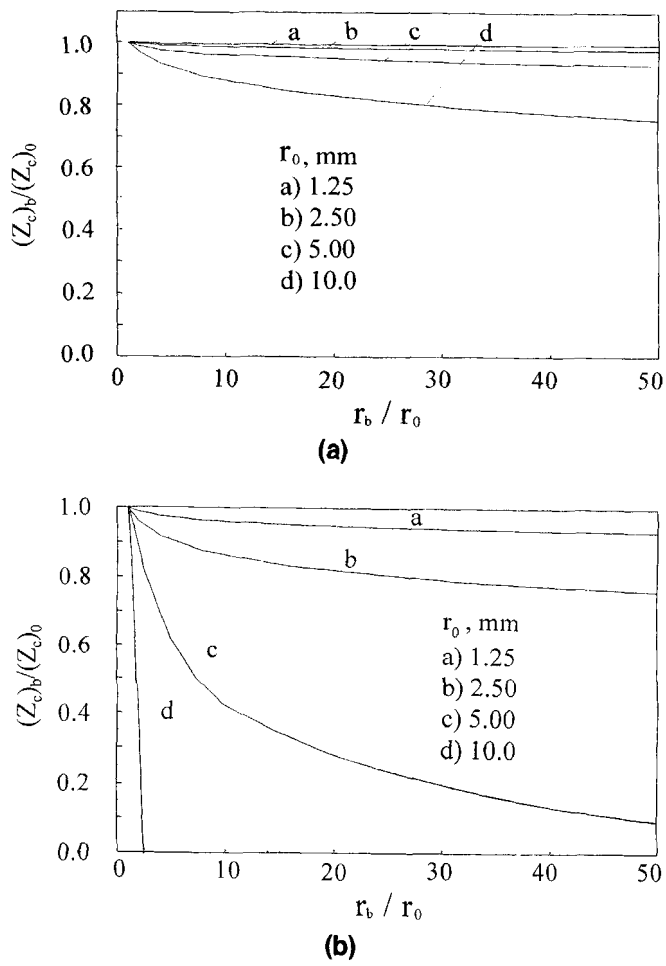

Figure 6. Effect of cylinder radius (r_0) on the relative critical heating rate $(Z_c)_b/(Z_c)_0$ for different values of r_b/r_0.

(a) $K_b = 10^{-13}$ m^2; (b) $K_b = 10^{-14}$ m^2.

exists no single equation which is generally applicable to powder assemblies. These equations are oversimplified for describing pore structure. Nevertheless, empirical equations can be obtained to calculate K_b for a particular powder with reasonable accuracy. For instance, an alumina powder (grade MA2LS ex. Alcan Chemicals, Gerrards Cross, U.K.) which has been used in model studies yields measured permeability coefficients (Bao and Evans, 1991) which give a reasonable fit with the following equation (German, 1987)

$$K_b = \frac{e^4 d^2}{90\,(1-e)^2}, \tag{22}$$

where d is the mean particle size and e is the porosity. If this is used as a powder bed, permeability coefficients of less than 10^{-14} m^2 would involve a packing efficiency of greater than 70% which is not attainable even for well compacted powder.

The results of the calculations are consolidated into a map (Figure 7). The curves represent the combinations of K_b and r_b/r_0 which give rise to 10% reduction of $(Z_c)_0$ [$(Z_c)_b/(Z_c)_0 = 0.9$]. Thus, an arbitrary 10% reduction in $(Z_c)_0$ is taken as a significant reduction in permissible heating rate brought

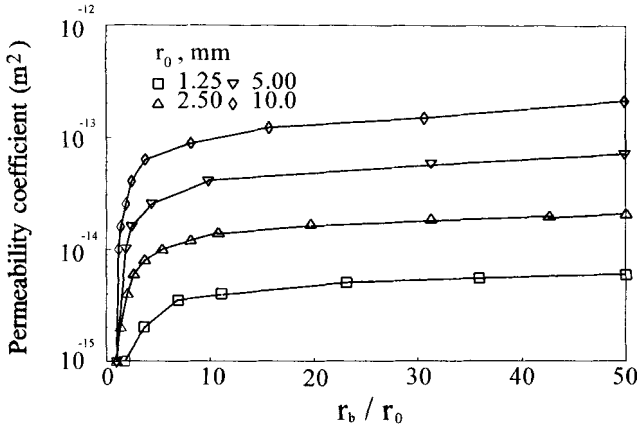

Figure 7. Combined effect of powder bed thickness (r_b) and its permeability coefficient (K_b) for cylinders with a range of radii.

Curves represent $(Z_c)_b/(Z_c)_0 = 0.9$.

about by the presence of the powder bed. Hence, in the area under the curves, the powder bed has a significant effect on the critical heating rate while above the curves, the powder bed effect is negligible.

Some generality in the prediction of the effects of powder beds by this model is lost by the fact that the material properties used in the calculations are for a system that necessarily produces a low critical rate of heating and, *ipso facto*, a low flux. Polyalphamethylstyrene would not normally be used on its own as an organic vehicle. The addition of low molecular weight constituents would increase the diffusion coefficient for degradation products in the solution through free volume effects, widen the decomposition temperature range and hence reduce $\dot{Q}$ for the same heating rate, or emerge early during the thermolysis to enhance porosity. In commercial systems, blends of polymers, waxes, plasticizer, and processing aids are used for these purposes (Edirisinghe and Evans, 1986).

In a commercial organic blend which could tolerate a higher heating rate, the flux would increase since

$$\frac{dv}{dt} \propto Z \frac{dh}{dT} \tag{23}$$

and for a given size of molding, a higher powder bed permeability coefficient and a thinner powder bed would be needed. The flux is inversely proportional to the molecular weight of the degradation product (Eq. 15). Thus a low molecular weight gas produces a high flux, but is also likely to have a higher diffusion coefficient in the polymer-ceramic suspension and a lower enthalpy of vaporization.

Conclusions

This model investigates the relative importance of the combined resistances to mass transport of polymer degradation products from a molding consisting of powder dispersed in an organic vehicle a) by diffusion in the binary polymer-powder suspension, and b) by permeation in a surrounding and supporting powder bed. It predicts the incidence of defects at the center of the molding in terms of the resistances. The conclusions are condensed into the form of a map for the ceramic-polymer system used, each line of which represents a different size of molding and defines the region where the powder bed has a significant effect on the critical rate of heating needed to prevent defect formation. Thus, for a given size of molding the minimum permeability coefficient for the powder bed and its maximum thickness can be deduced.

Acknowledgments

EPSRC in the U.K. is thanked for financial support for this work under grant No. GR/H 93545.

Notation

$C, C_{i,j}$ = concentration of monomer in solution in the polymer phase based on the total volume of suspension and at $r = i\Delta r$, $t = j\Delta t$, kg·m^{-3}
E = activation energy for thermal degradation, J·mol^{-1}
ΔH_{vap} = enthalpy of vaporization, J·mol^{-1}
h = fraction of mass of polymer remaining, $0 < h < 1$
i = node number for radius
I = constant in Eq. 21, Pa
K_0 = specific rate constant for thermal degradation, s^{-1}
M = total number of time steps
p_0^1 = vapor pressure of monomer over the pure liquid, Pa
R = gas constant, J·mol^{-1}·K^{-1}
$T_0, \Delta T$ = initial temperature, K, and temperature step
v = volume of degradation product displaced from molding per unit area, m
V_f = average hole-free volume per unit mass, m^3·kg^{-1}
$V_1(0)$ = specific volume of monomer at 0 K, m^3·kg^{-1}
$V_2(0)$ = specific volume of polymer at 0 K, m^3·kg^{-1}
V_p = volume fraction in polymer-powder system, $0 < V_p < 1$
W_2 = weight fraction of polymer in polymer-monomer solution, $0 < W_2 < 1$
Z_1, Z_2 = the lower and upper limits for searching the critical heating rate, K·s^{-1}
$(Z_c)_b$ = critical heating rate with powder bed, K·s^{-1}
$(Z_c)_0$ = critical heating rate without powder bed, K·s^{-1}

Greek letters

α = coefficient in Eq. 4
β = coefficient in Eq. 4
γ = coefficient in Eq. 4
η = viscosity of vapor in Eq. 14, Pa·s
ξ = ratio of critical molar volumes of hopping units of monomer and polymer in Eq. 2
ρ_p = density of polymer, kg·m^{-3}
ζ = constant in Eq. 15, m^3·K^{-1}·mol^{-1}
ϕ = volume fraction of monomer in polymer in Eq. 2, $0 < \phi < 1$
χ = interaction parameter for polymer-monomer system in Eq. 2
ϵ = tolerance for critical heating rate search
ω = overlap factor for free volume in Eq. 2

Literature Cited

Bao, Y., and J. R. G. Evans, "Kinetics of Capillary Extraction of Organic Vehicle from Ceramic Bodies: I Flow in Porous Media," *J. Euro. Ceram. Soc.*, **8**, 81 (1991).

Birch, G. A., *Molecular Gas Dynamics*, Claredon Press, Oxford, U.K. p. 73 (1976).

Bondi, A. A., and D. J. Simkin, "A Corresponding-States Correlation for Higher Molecular-Weight Liquids," *AIChE J.*, **6**, 191 (1960).

Calvert, P., and M. Cima, "Theoretical Models for Binder Burnout," *J. Amer. Ceram. Soc.*, **73**, 575 (1990).

Canagaratne, S. G., D. Margerison, and J. P. Newport, "Thermodynamics of Solutions of Polymers of α-Methylstyrene in α-Methylstyrene and Cumene," *Trans. Farad. Soc.*, **62**, 3058 (1966).

Cass, R. B., "Fabrication of Continuous Ceramic Fiber by the Viscous Suspension Spinning Process," *Bull. Amer. Ceram. Soc.*, **70**, 424 (1991).
Coulter, K. E., and H. Kehde, "Styrene Polymers. Monomers," *Encyclopedia of Polymer Science and Technology*, H. F. Mark and N. G. Gaylord, eds., Interscience, New York, p. 152 (1970).
Duda, J. L., Y. C. Ni, and J. S. Vrentas, "Diffusion of Ethylbenzene in Molten Polystyrene," *J. Appl. Poly. Sci.*, **22**, 689 (1978).
Duda, J. L., J. S. Vrentas, S. T. Ju, and H. T. Liu, "Prediction of Diffusion Coefficients for Polymer-Solvent Systems," *AIChE J.*, **28**, 279 (1982).
Edirisinghe, M. J., and J. R. G. Evans, "Review: Fabrication of Engineering Ceramics by Injection Moulding," *Int. J. High. Tech. Ceram.*, **2**, 1 (1986).
Endo, H., T. Fujimoto, and M. J. Nagasawa, "Volume Recovery of Glassy Poly (α-Methylstyrene)," *J. Poly. Sci.*, **7**, Part a-2, 1669 (1969).
Evans, J. R. G., M. J. Edirisinghe, J. K. Wright, and J. Crank, "On the Removal of Organic Vehicle from Moulded Ceramic Bodies," *Proc. Roy. Soc. Lond.*, **A432**, 321 (1991).
Forsythe, G. E., and C. B. Moler, *Computer Solution of Linear Algebraic Systems*, Prentice-Hall, Englewood Cliffs, N.J., p. 114 (1967).
German, R. M., "Theory of Thermal Debinding," *Int., J. Powder Met.*, **23**, 237 (1987).
Greener, J., and J. R. G. Evans, "The Film Blowing of Ceramics," *J. Mat. Sci.*, **28**, 6190 (1993).
Hammond, P. D., and J. R. G. Evans, "On the Blow Moulding of Ceramics," *J. Mat. Sci. Lett.*, **10**, 294 (1991).
Haunton, K. M., J. K. Wright, and J. R. G. Evans, "The Vacuum Forming of Ceramics," *Br. Ceram. Trans. J.*, **89**, 53 (1990).
Maddox, R. N., and A. L. Hines, *Mass Transfer Fundamentals and Applications*, Prentice-Hall, Englewood Cliffs, NJ, p. 151 (1985).
Matar S. A., M. J. Edirisinghe, J. R. G. Evans, and E. H. Twizell, "The Effect of Porosity Development on the Removal of Organic Vehicle from Ceramic and Metal Mouldings," *J. Mat. Res.*, **8**, 617 (1993).
Matar, S. A., M. J. Edirisinghe, J. R. G. Evans, E. H. Twizell, and J. H. Song, "Modelling of the Removal of Organic Vehicle from Ceramic or Metal Mouldings: The Effect of Gas Permeability on the Incidence of Defects," *J. Mat. Sci.*, **30**, 3085 (1995).
Matar, S. A., M. J. Edirisinghe, J. R. G. Evans, and E. H. Twizell, "Diffusion of Degradation Products in Ceramic Mouldings During Pyrolysis: Effect of Geometry," *J. Amer. Ceram. Soc.*, in press (1996).
Press, W. H., B. P. Flannery, S. A. Teukolsky, and W. T. Vetterling, *Numerical Recipes*, Cambridge Univ. Press, London, p. 277 (1986).
Reich, L., and S. S. Stivala, *Elements of Polymer Degradation*, McGraw-Hill, New York, p. 92 (1971).
Richerson, D. W., *Modern Ceramic Engineering*, 2nd ed., Marcel Dekker, New York, p. 471 (1992).
Scheidegger, A. E., *The Physics of Flow Through Porous Media*, 3rd ed., Univ. of Toronto Press, Canada, p. 152 (1975).
Shaw, H. M., and M. J. Edirisinghe, "A Model for the Diffusion of Organic Additives During Thermolysis of a Ceramic Body," *Phil. Mag., A.*, **72**, 267 (1995).
Twizell, E. H., *Computational Methods for Partial Differential Equations*, Chap. 5, Ellis Horwood, Chichester, U.K. (1984).
Wright, J. K., J. R. G. Evans, and M. J. Edirisinghe, "Degradation of Polyolefin Blends Used for Ceramic Injection Moulding," *J. Amer. Ceram. Soc.*, **72**, 1822 (1989).
Wright, J. K., R. M. Thomson, and J. R. G. Evans, "On the Fabrication of Ceramic Windings," *J. Mat. Sci.*, **25**, 149 (1990).
Zhang, J. G., M. J. Edirisinghe, and J. R. G. Evans, "A Catalogue of Ceramic Injection Moulding Defects and Their Causes," *Ind. Ceram.*, **9**, 72 (1989).

Appendix: Computing Scheme

The following procedure is used in the search for Z_c:

- Input polymer and monomer parameters.
- Input the number of nodes for time and radius space M and N, respectively.
- Input time and temperature steps Δt and ΔT.
- Input the powder volume fraction in the molding V_c.
- Input the permeability coefficient of the powder bed K_b.
- Input the radius of the cylinder r_0 and powder bed r_b.
- Input the region for the critical heating rate search $[Z_1, Z_2]$.

Search for Z_c, select a heating rate Z in region $[Z_1, Z_2]$ using the gold-sectioning method; calculate $\dot{Q}$ at each temperature; and set initial concentration $C_{i,0} = 0$.

For each $j = 1$, calculate D (Eq. 2) based on the initial concentration and solve Eq. 4 using boundary condition $C_{N,0} = 0$.

For time steps $j = 2, 3, \ldots$, calculate the mass displaced w_{j-1} (Eq. 16), viscosity η_{j-1} (Eq. 17), and pressure developed at the boundary p_j, and then solve Eq. 20 for θ_1. Subsequently, convert pressure to boundary concentration $C_{N,j}$ (Eq. 19); calculate D based on concentration and temperature at time level $j-1$ (Eq. 2); solve system of equations (Eq. 4) for concentration profile; and then convert central concentration of monomer $C_{0,j}$ to central vapor pressure. Finally, check whether the central vapor pressure is greater than ambient pressure (boiling criterion) and whether critical heating, $(Z_2 - Z_1)/Z < \epsilon$; adjust Z_1 and Z_2 to reduce the search region. Repeat the above procedures until both above thresholds are satisfied.

Manuscript received June 9, 1995, and revision received Sept. 20, 1995.